Article

Fossil evidence for a pharyngeal origin of the vertebrate pectoral girdle

https://doi.org/10.1038/s41586-023-06702-4

Received: 14 April 2023

Accepted: 2 October 2023

Published online: 1 November 2023

Open access

Check for updates

Martin D. Brazeau[1,2]✉, Marco Castiello[1,7], Amin El Fassi El Fehri[1,8], Louis Hamilton[1], Alexander O. Ivanov[3,4], Zerina Johanson[2] & Matt Friedman[2,5,6]

The origin of vertebrate paired appendages is one of the most investigated and debated examples of evolutionary novelty[1–7]. Paired appendages are widely considered as key innovations that enabled new opportunities for controlled swimming and gill ventilation and were prerequisites for the eventual transition from water to land. The past 150 years of debate[8–10] has been shaped by two contentious theories[4,5]: the ventrolateral fin-fold hypothesis[9,10] and the archipterygium hypothesis[8]. The latter proposes that fins and girdles evolved from an ancestral gill arch. Although studies in animal development have revived interest in this idea[11–13], it is apparently unsupported by fossil evidence. Here we present palaeontological support for a pharyngeal basis for the vertebrate shoulder girdle. We use computed tomography scanning to reveal details of the braincase of *Kolymaspis sibirica*[14], an Early Devonian placoderm fish from Siberia, that suggests a pharyngeal component of the shoulder. We combine these findings with refreshed comparative anatomy of placoderms and jawless outgroups to place the origin of the shoulder girdle on the sixth branchial arch. These findings provide a novel framework for understanding the origin of the pectoral girdle. Our evidence clarifies the location of the presumptive head–trunk interface in jawless fishes and explains the constraint on branchial arch number in gnathostomes[15]. The results revive a key aspect of the archipterygium hypothesis and help reconcile it with the ventrolateral fin-fold model.

The two major theories of the origin of vertebrate appendages differ in their ability to explain evolutionary patterns. The ventrolateral fin-fold hypothesis proposes that paired fins arose from ventrolateral keels extending the length of the trunk, which became subdivided into pectoral and pelvic fins. The archipterygium hypothesis argues that the girdles derived from an ancestral skeletal gill arch and that the fin endoskeleton formed from gill rays. The fin-fold hypothesis is seen as the more 'successful' of the two theories[4,16], with support from developmental genetics[17] and widespread evidence of stem-group gnathostomes possessing ventrolateral fin folds in some form[5,7]. However, the fin-fold hypothesis does not explain the origin of the pectoral girdle, which resulted in the subdivision of the head into a separate skull and shoulder. Furthermore, it predicts the simultaneous origin of pectoral and pelvic fins, which is currently contradicted by fossil data[5,7]. The archipterygium hypothesis explains the pectoral girdle and separate origins of pectoral and pelvic fins by basing their origins on pre-existing structures. Clues from developmental genetics[11–13] have renewed interest in the archipterygium hypothesis as a viable theory.

A key challenge to testing the archipterygium hypothesis with evidence from the fossil record is the rarity of fossilized gill arches. Gill arches are cartilage-derived endoskeletal structures that were either unossified or weakly ossified and are therefore not preserved in the earliest fossil taxa. The closest fossil sister group of jawed vertebrates is the Osteostraci, which ranges from the Wenlock epoch of the Silurian period to the Late Devonian period (approximately 432 to 378 million years ago (Ma)). Osteostracans possessed distinct pectoral fins, but these were attached to a unified craniothoracic block of cartilage that was surmounted by tessellated dermal bone. Fossilized pharyngeal arches are completely unknown in osteostracans, obscuring reconstructions of pharyngeal conditions[18] preceding the origins of jaws and a pectoral girdle. The phylogenetically earliest jawed vertebrates are the placoderms, heavily armoured predatory fishes and contemporaries of osteostracans. Placoderm gill arches are rarely preserved and incompletely understood[19,20]. However, a crucial piece of evidence has long been overlooked. Despite the rarity of the arches themselves, their attachments are well-preserved as discrete facets near the perimeter of well-ossified braincases of both osteostracans and placoderms[18]. In osteostracans, however, the articulation facets are quite remote from the core of the braincase, situated near the perimeter of a broad cephalic shield that defines an enlarged oralobranchial chamber (see below). Alongside these are well-established anatomical landmarks in the form of cranial innervation and blood supply patterns, recorded as grooves or ossified canals within these braincases and consistent across vertebrates. This record of both hard and inferred soft-tissue anatomy provides a framework for investigating the role of the pharynx in the

[1]Department of Life Sciences, Imperial College London, Ascot, UK. [2]The Natural History Museum, London, UK. [3]Department of Sedimentary Geology, Institute of Earth Sciences, St Petersburg State University, St Petersburg, Russia. [4]Institute of Geology and Petroleum Technologies, Kazan Federal University, Kazan, Russia. [5]Museum of Paleontology, University of Michigan, Ann Arbor, MI, USA. [6]Department of Earth and Environmental Sciences, University of Michigan, Ann Arbor, MI, USA. [7]Present address: London Academy of Excellence, London, United Kingdom. [8]Present address: Paläontologisches Institut und Museum, Universität Zürich, Zurich, Switzerland. ✉e-mail: m.brazeau@imperial.ac.uk

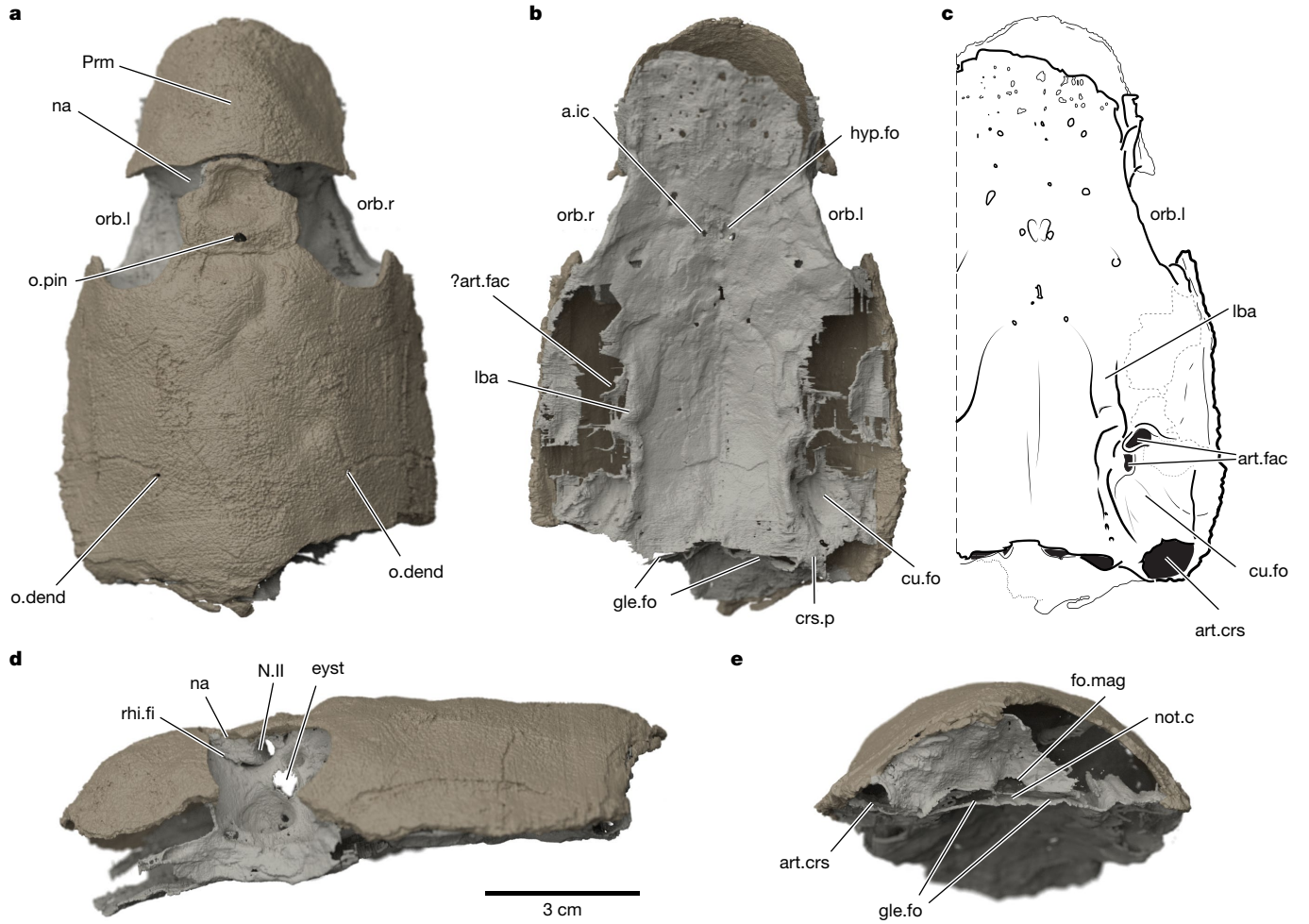

Fig. 1 | The braincase and skull roof of *K. sibirica* Bystrow 1956 specimen TsNIGR 7656 as a virtual three-dimensional rendering. a, Dorsal view. **b**, Ventral view. **c**, Interpretive illustration of ventral view. **d**, Left lateral view. **e**, Posterior view. a.ic, foramen for internal carotid artery; art.crs, articular facet on end of craniospinal process; art.fac, articular facets for branchial arches; crs.p, craniospinal process; cu.fo, cucullaris muscle fossa; eyst, eystalk attachment; fo.mag, foramen magnum; gle.fo, fossa for occipital glenoid facets; hyp.fo, hypophyseal fossa; lba, laterobasal angle; N.II, optic tract canal; na, naris; not.c, notochordal canal; o.dend, endolymphatic duct opening; o.pin, pineal opening; orb.l, left orbit; orb.r, right orbit; Prm, premedian plate; rhi.fi, rhinocapsular fissure. Dark beige material is dermal (exoskeletal) bone and light beige material is perichondral (endoskeletal) bone.

skeletal and bodyplan transformations leading to the origin of paired pectoral fins and a distinct pectoral girdle.

The type and only specimen of *K. sibirica* (FN Chernyshev Central Research Geological Museum in St Petersburg, Russia, TsNIGR 7656) is a three-dimensionally preserved skull roof and braincase (Fig. 1). The skull of *Kolymaspis* is anteroposteriorly elongate, with a pronounced premedian 'snout' (upper lip, sensu ref. 21) and large, dorsolaterally directed orbits. The dermal skull roof is nearly complete, with the separately ossified rostropineal plate and rhinocapsular ossification in articulation (Fig. 1). The dermal skull roof is coated in stellate tubercles, consistent with 'acanthothoracid' placoderms[22–24]. In ventral view, the braincase is broad and deeply concave; the parachordal region is laterally demarcated by raised longitudinal crests (laterobasal angles; Fig. 1). The parachordal plates here terminate posteriorly without forming a marked occipital process; the occipital glenoid facets (attachments to the spinal column) were flush with the posterior margin of the braincase, in a condition similar to *Brindabellaspis*[25,26]. They are wide, dorsoventrally flat, openings flanking the notochordal canal. Posteriorly, the braincase flares laterally into stout craniospinal processes (Fig. 1). This process is most complete on the left (observer right) side. The distal part of the craniospinal process is an open, rimmed facet (Fig. 1), indicating it was the articulation point for a second cartilage. This corresponds with *Brindabellaspis*, which also has a terminal facet on the craniospinal process[25] (Extended Data Fig. 1). However, this feature is unknown in any other placoderms, in which the facet is either absent and the craniospinal process is wholly covered in perichondral bone (as in *Romundina*; Fig. 2c), or capped in dermal bone as in arthrodires. In posterior view, the occipital surface also resembles *Brindabellaspis* in being broad, centrally concave and lacking identifiable cavities for paired epaxial musculature (muscles raising the skull). The foramen magnum is nearly twice the diameter of the notochordal canal, consistent with stem-group gnathostome conditions, and the two are contiguous openings positioned near the ventral margin of the braincase (Fig. 1).

These observations of the *Kolymaspis* braincase and comparisons to other taxa enable us to identify the ancestral position of head–shoulder separation in jawless fishes and propose specific musculoskeletal transformations in the origin of the gnathostome pectoral girdle. The placoderm craniospinal processes articulate with the pectoral girdle (shld.grd; Fig. 2). The open articular facet on the craniospinal process of *Kolymaspis* and *Brindabellaspis* (hereafter referred to collectively as brindabellaspidids[25]) points to an endoskeletal element here, forming a junction with the pectoral girdle. This is notable because this endoskeletal element would lie in series with the pharyngeal arches

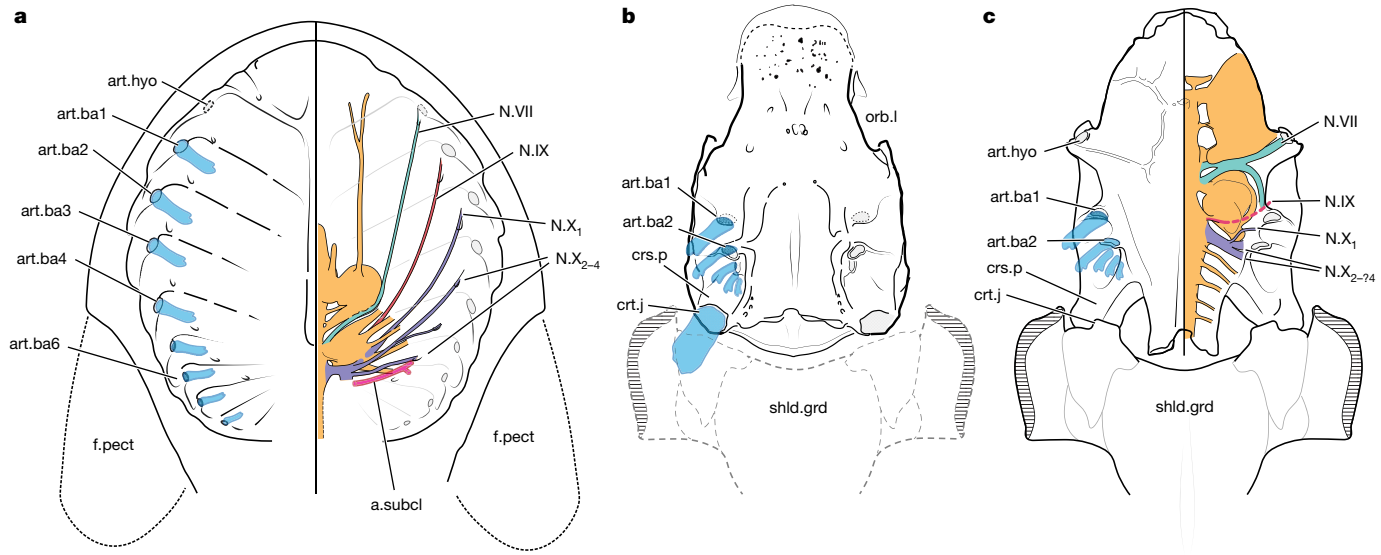

Fig. 2 | Comparative anatomy of cranial processes and branchial arch attachments in stem gnathostomes. a, Osteostracan *Nectaspis* (composite based on ref. 47). **b**, Acanthothoracid placoderm *Kolymaspis*. **c**, Acanthothoracid placoderm *Romundina* (original based on data from ref. 48 and new data). Transparent blue structures represent reconstructed branchial arches. art. ba1–6, serially numbered branchial arch attachments (corresponds to art.fac in Fig. 1); art.hyo, hyoid arch articulation; a.subcl, canal for subclavian artery; crt.j, craniothoracic joint; f.pect, pectoral fin; N.VII, facial nerve canal; N.IX, glossopharyngeal canal; $N.X_{1-4}$, vagus nerve canal branches (numbered 1–4); shld.grd, shoulder girdle. Not to scale.

(Fig. 2) and a key anatomical landmark of the head–shoulder boundary in gnathostomes: the cucullaris muscle, responsible for depressing the skull towards the shoulder girdle[27–29]. There is a wealth of anatomical and developmental evidence that the cucullaris muscle is of branchial origin[16,30–32]. This gives rise to the prediction that it may have ancestrally joined a branchial arch. We propose that this endoskeletal element is a serial homologue of an upper branchial element (epibranchial or pharyngobranchial, given its topological position) and therefore that the shoulder girdle of these taxa incorporated the dorsal element of a gill arch. Although placoderm braincases possess only two clear articular facets for branchial arches, rare skeletal material shows that they possess at least five skeletal arches (the posteriormost arch may be specialized, as in some chondrichthyans)[20]. No placoderms are known to possess more than this number of arches. This anatomical interpretation implies that the sixth branchial arch would most probably have been the one incorporated into the pectoral girdle, if our interpretation is correct.

The sixth branchial arch is key in comparisons with jawless outgroups and enables independent support of our topological observations. Osteostracans differ from all known jawed vertebrates in the absence of a distinct head–shoulder separation, which is generally regarded as the ancestral gnathostome condition[27,28]. There are also no obvious points of homology that mark this separation in osteostracans. However, our hypothesis locates this presumptive division at the level of the sixth branchial arch. Notably, osteostracans frequently preserve a canal for the subclavian artery, the main arterial branch that supplies the pectoral fins. This artery stems from a cluster of arteries supplying the most posterior efferent branchial arteries serving the posterior pharyngeal arches[18,33,34]. The main trunk of the subclavian artery is seen in several specimens, showing that it extends along the interbranchial ridge of the sixth and seventh branchial arches[33,34] (Fig. 2a and Extended Data Fig. 2). Locating the shoulder on the sixth branchial arch also provides a precise explanation for a puzzling phenomenon in which most gnathostomes appear to be constrained to no more than five gill arches (hexanchiform sharks notwithstanding—these appear to involve duplication of an intermediate arch[35]), whereas jawless fishes range from five to several dozen separate gill compartments[15]. If the ancestral pectoral girdle incorporated the sixth branchial arch, this would strongly bias the standard complement of jawed vertebrate arches to no more than five.

These observations in a phylogenetic context (Fig. 3 and Extended Data Figs. 3 and 4) enable us to propose a new hypothesis for the origin of the pectoral girdle. We propose that the pectoral girdle is established on the position of the sixth branchial arch in the jawless ancestor of jawed vertebrates, and that this structure formed the primary basis of a separate head and shoulder. The initial incorporation of the gill arch provided support for the rear wall of the pharynx, joined to the skull by a kinetic, moveable linkage (Fig. 3). This link persisted in placoderms as a craniothoracic joint, and in some taxa (such as the brindabellaspidids) a vestige of the endoskeletal component remained (Fig. 3). In modern gnathostomes, the endoskeletal elements of this sixth branchial arch are completely lost (see next paragraph on origin of scapulocoracoid). However, exoskeletal (dermal) components of the pectoral girdle (for example, cleithrum and clavicle) may have their origins from branchiomeric dermal plates covering this arch (that is, from a branchial operculum). Evidence from *Romundina* indicates that some placoderms possessed dermal branchial coverings posterior to the submarginal plate, which is the main opercular bone in placoderms (Extended Data Fig. 5). A similar condition is possible in the enigmatic new taxon *Xiushanosteus* from the early Silurian of China[36]. If one reinterprets the larger, more posterior post-suborbital plate in *Xiushanosteus* as a submarginal, then the smaller plate originally identified as a submarginal becomes a posterior submarginal similar to *Romundina*.

We can tentatively suggest new points of homology between the heads of osteostracans and jawed vertebrates and suggest specific skeletal transformations that occurred during the origin of the pectoral girdle. First, the postbranchial lamina (rear wall of the gill chamber) is a putative homologue of a plate of branchial association (Fig. 3); this is consistent with its position and demonstrated ability to support development of tooth-like denticles[37], suggesting that it at least partly derives from cranial neural crest[28]. The formation of a postbranchial lamina occurred as the gill openings changed from pore-like openings of jawless fishes into deep-sided clefts of jawed taxa. This was concomitant with changes to the structure of the braincase, in which the broad lateral brim was withdrawn medially, exposing the expanded clefts laterally. The sixth arch lost respiratory tissue (gills) and became the

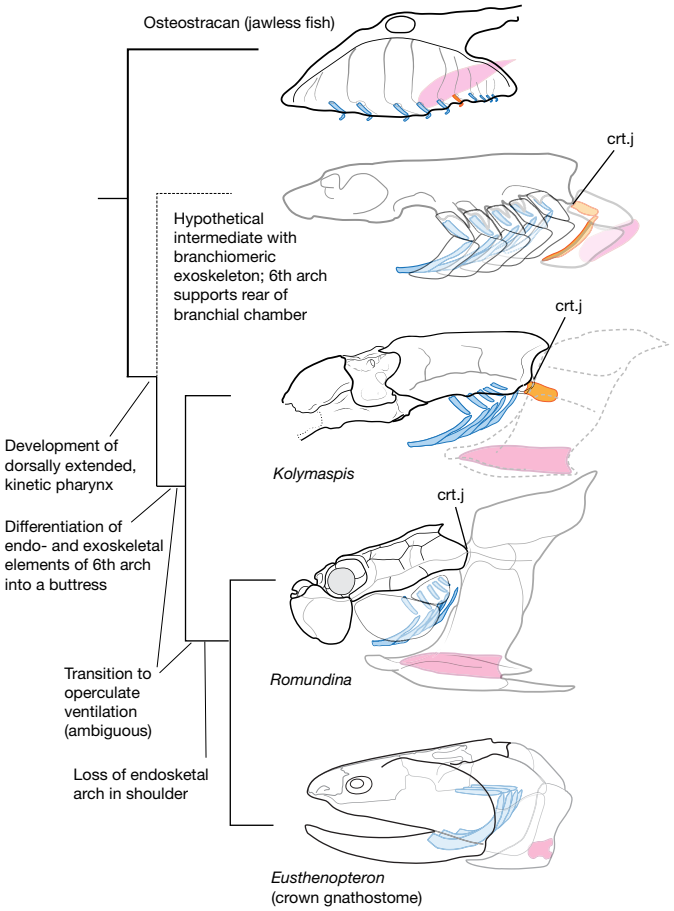

Fig. 3 | Summary phylogeny of early gnathostomes with reconstructions to show comparative anatomy of pharyngeal arches and shoulder linkages. Hypothetical intermediate is shown, for clarity of comparative anatomy; specific geometries may have varied substantially. Gill arch morphologies in osteostracan and placoderms are hypothetical and are shown to indicate location of articulations and constraints on overall pharynx architecture. Blue, branchial arches; orange, sixth branchial or thoracic arch; pink, pectoral fin attachment or scapulocoracoid. See Supplementary Information for complete phylogeny. Dashed lines indicate inferred pectoral girdle. Osteostracan is a composite based on ref. 47; *Romundina* is based on ref. 49 and new data; *Eusthenopteron* is a composite based on ref. 50.

basis of a craniothoracic joint supporting feeding or buccal pumping. We do not necessarily invoke the gill arches as the anatomical precursor of the pectoral fin skeleton or the scapulocoracoid, as predicted by the archipterygium hypothesis. Recent fate-mapping studies in skate (Chondrichthyes) show that the scapulocoracoid is composed of trunk mesoderm[13] (compared to a zone of mixed cranial neural crest and trunk mesoderm in the gill arches). Additionally, a pectoral fin and proximal attachment was already present and anatomically separate from the gill arches in the osteostracans. Gill arches and pectoral elements thus fail the conjunction test of homology. Nevertheless, the close anatomical proximity of these structures would have allowed them to join a common dermal support (Fig. 3).

Our hypothesis partly revives the archipterygium hypothesis, but not as originally envisioned by Gegenbaur[8]. There is no known fossil evidence of a direct skeletal remnant of the ancestral gill arch in crown-group gnathostomes, only traces in the form of patterns of vascularization and musculature inherited from jawless ancestors[28]. Notably, the last direct vestiges of a pharyngeal arch in the shoulder girdle would have been lost in placoderms (Fig. 3), with evidence seen only in the enigmatic brindabellaspidids as described above. There is no requirement in our hypothesis, however, for either the scapulocoracoid or the pectoral fin endoskeleton to be of pharyngeal origin, as in Gegenbaur's archipterygium. A separate head–girdle instead evolved as part of changes in the architecture of the pharynx, rather than primarily to support fins. Our work arrives independently at a previous suggestion that the pectoral girdle and fin are a morphological amalgam of cranial and thoracic regions of the body[16]. Fossil evidence for this has previously been suggested by Zangerl[38]. However, as with Gegenbaur's original theory, Zangerl's idea relied heavily on chondrichthyan anatomy[38], referencing symmoriids and iniopterygians. These taxa are increasingly demonstrated as highly nested within chondrichthyans and well removed from the origin of gnathostomes[39,40], casting doubt on their value as models for ancestral jawed vertebrates. Thus, elements of both the archipterygium and the fin-fold hypotheses are combined to explain the origin of pectoral appendages, the shoulder and a distinct gnathostome head as a total system. All these conclusions could potentially be tested by fate-mapping studies in modern osteichthyans (as these taxa retain the dermal pectoral girdle) as well as through new fossil finds of early gnathostomes.

This interpretation adds important functional details to the tight phylogenetic connection between the origin of a pectoral girdle and the origin of jaws. The craniospinal process is one of the pivot points in the four-bar linkage that makes up the placoderm jaw-closing apparatus[41]. This suggests that as a sixth branchial arch became established as the rearmost support and a kinetic joint, tying the origin of the pectoral girdle to a suite of changes to the pharynx involved in opening and closing the mouth and throat. Recent evidence suggests a compact, operculate pharynx as the ancestral condition for gnathostomes[42], rather than the historically accepted shark-like septate model. Thus, it is reasonable to conclude that the origin of the pectoral girdle is integrated with the evolution of a compact bucco-pharyngeal apparatus for efficient gill ventilation or feeding.

Our hypothesis is testable on several lines of evidence that could eventually overturn it. We discuss these along with existing points of weakness. First, it depends on the resolution of either *Kolymaspis* or *Brindabellaspis* as the sister group taxa of all other jawed vertebrates, and thus rests on the hypothesis of placoderm paraphyly. This is currently the case in our phylogeny (Extended Data Fig. 6). However, statistical support for placoderm paraphyly is weak (see bootstrap values in Extended Data Fig. 3) and highly debated[43,44]. Under placoderm monophyly, our hypothesis depends at least on the phylogenetic mapping of the craniothoracic facet to the base of all jawed vertebrates. We conducted additional analyses with constraints on placoderm monophyly leading to equivocal support for our new hypothesis (Extended Data Fig. 6 and Supplementary Information). Thus, new phylogenetic tests could reveal that the condition in the brindabellaspidids is uniquely derived (that is, neomorphic). The discovery of new fossils with both supernumerary branchial arches and a discrete pectoral girdle would also challenge our hypothesis. Furthermore, an alternative interpretation of the articular facet in brindabellaspidids is that it represents a connection to a shoulder cartilage not of pharyngeal origin. In our view, these explanations are less parsimonious and do not help account for the branchiomeric derivation of the cucullaris muscle, but they could be supported by future fossil discoveries or phylogenetic analyses. Even if those specifics are rejected, our hypothesis adds important new comparative anatomical perspectives that better reconcile the disparate anatomies of osteostracans and placoderms.

Our proposal synthesizes findings from the past two decades of research into the origin of the pectoral girdle. Furthermore, it clarifies key questions of comparative anatomy that have impeded studies on the origin of the vertebrate neck and shoulders. Key among these is resolution of the identity and location of the cucullaris muscle in osteostracans, a crucial anatomical landmark in establishing the head–shoulder interface[27–29,45]. Previous studies have struggled to identify the location of the cucullaris in osteostracans, concluding that it was

absent[27] or placing it in an epaxial location[46]. We argue that it was an undifferentiated branchial levator or protractor muscle and would have been housed in the perimeter of the oralobranchial chamber. This morphology is topologically consistent with placoderm braincases which show that the cucullaris muscle is serially aligned with the branchial levator muscles. Our investigation suggests it derived from the sixth branchial levator, consistent with the predictions of recent comparative developmental studies[29]. Despite the loss of posterior endoskeletal branchial arches in gnathostomes, a branchiomeric muscle of the sixth branchial arch (as the cucullaris muscle) maintained a consistent topological relationship with the dermal exoskeleton (Fig. 3). This new model of musculoskeletal transformation in pectoral girdle origins thus unifies a wide array of evidence on the origin of the pectoral girdle. It adds important new details to the biomechanical basis for the origin of the girdle and clarifies the comparative anatomy of key jawless and jawed fishes. This new framework is consistent with recent proposals of a dual origin of the pectoral girdle[16] and thus contributes to the reconciliation of two long-debated theories of paired fin origins.

Online content

Any methods, additional references, Nature Portfolio reporting summaries, source data, extended data, supplementary information, acknowledgements, peer review information; details of author contributions and competing interests; and statements of data and code availability are available at https://doi.org/10.1038/s41586-023-06702-4.

1. Shubin, N., Tabin, C. & Carroll, S. Fossils, genes and the evolution of animal limbs. *Nature* **388**, 639–648 (1997).
2. Shubin, N., Tabin, C. & Carroll, S. Deep homology and the origins of evolutionary novelty. *Nature* **457**, 818–823 (2009).
3. Wagner, G. P. *Homology, Genes, and Evolutionary Innovation* (Princeton Univ. Press, 2014).
4. Coates, M. The evolution of paired fins. *Theory Biosci* **122**, 266–287 (2003).
5. Wilson, M. V. H., Hanke, G. F. & Märss, T. in *Major Transitions in Vertebrate Evolution* (eds Anderson, J. S. & Sues, H.-D.) 122–149 (Indiana Univ. Press, 2007).
6. Johanson, Z. Evolution of paired fins and the lateral somitic frontier. *J. Exp. Zool. B* **314B**, 347–352 (2010).
7. Gai, Z. et al. Galeaspid anatomy and the origin of vertebrate paired appendages. *Nature* **609**, 959–963 (2022).
8. Gegenbaur, C. Zur morphologie der Gliedmaassen der Wirbeltiere. *Morphologisches Jahrbuch* **2**, 396–420 (1876).
9. Thacher, J. Median and paired fins: a contribution to the history of vertebrate limbs. *Trans. Connecticut. Acad. Sci.* **3**, 281–308 (1877).
10. Balfour, F. M. On the development of the skeleton of the paired fins of Elasmobranchii, considered in relation to its bearings on the nature of the limbs of the vertebrata. *Proc. Zool. Soc. Lon.* **49**, 656–670 (1881).
11. Tabin, C. J. Why we have (only) five fingers per hand: Hox genes and the evolution of paired limbs. *Development* **116**, 289–296 (1992).
12. Gillis, J. A., Dahn, R. D. & Shubin, N. H. Shared developmental mechanisms pattern the vertebrate gill arch and paired fin skeletons. *Proc. Natl Acad. Sci. USA* **106**, 5720–5724 (2009).
13. Sleight, V. A. & Gillis, J. A. Embryonic origin and serial homology of gill arches and paired fins in the skate, *Leucoraja erinacea*. *eLife* **9**, e60635 (2020).
14. Bystrow, A. *Kolymaspis sibirica* g. n., s. n.—a new representative of the Lower Devonian agnathous vertebrates. *Vestnik Leningr. Univ. Geol. Geogr.* **18**, 5–13 (1956).
15. Janvier, P. in *Recent Advances in the Origin and Early Radiation of Vertebrates* (eds Arratia, G., Wilson, M. V. H. & Cloutier, R.) 29–52 (Verlag Dr. Friedrich Pfeil, 2004).
16. Diogo, R. Cranial or postcranial—Dual origin of the pectoral appendage of vertebrates combining the fin-fold and gill-arch theories? *Dev. Dyn.* **249**, 1182–1200 (2020).
17. Tanaka, M. et al. Fin development in a cartilaginous fish and the origin of vertebrate limbs. *Nature* **416**, 527–531 (2002).
18. Janvier, P. *Les Céphalaspides du Spitsberg* (Éditions du Centre National de la Recherche Scientifique, 1985).
19. Stensiö, E. A. in *Traité de Paléontologie*, Vol. 4 (ed. Piveteau, J.) 71–692 (1969).
20. Brazeau, M. D., Friedman, M., Jerve, A. & Atwood, R. C. A three-dimensional placoderm (stem-group gnathostome) pharyngeal skeleton and its implications for primitive gnathostome pharyngeal architecture. *J. Morphol.* **278**, 1220–1228 (2017).
21. Dupret, V., Sanchez, S., Goujet, D., Tafforeau, P. & Ahlberg, P. E. A primitive placoderm sheds light on the origin of the jawed vertebrate face. *Nature* **507**, 500–503 (2014).
22. Ørvig, T. in Problèmes Actuels de Paléontologie: Evolution des Vertébrés (ed. Lehman, J. P.) 41–72 (Colloques Internationaux Centre National de la Recherche Scientifique, 1975).
23. Stensiö, E. A. Contributions to the knowledge of the vertebrate fauna of the Silurian and Devonian of western Podolia. II. Notes on two arthrodires from the Downtonian of Podolia. *Arkiv. Zoolog.* **35A**, 9 (1944).
24. Long, J. A. & Young, G. C. Acanthothoracid remains from the Early Devonian of New South Wales, including a complete sclerotic capsule and pelvic girdle. *Mem. Assoc. Australas. Palaeontol.* **12**, 65–80 (1998).
25. Young, G. C. A new Early Devonian placoderm from New South Wales, Australia, with a discussion of placoderm phylogeny. *Palaeontographica* **167**, 10–76 (1980).
26. Zhu, Y.-A. et al. Endocast and bony labyrinth of a Devonian "placoderm" challenges stem gnathostome phylogeny. *Current Biology* **31**, 1112–1118.e4 (2021).
27. Ericsson, R., Knight, R. & Johanson, Z. Evolution and development of the vertebrate neck. *J. Anat.* **222**, 67–78 (2012).
28. Matsuoka, T. et al. Neural crest origins of the neck and shoulder. *Nature* **436**, 347–355 (2005).
29. Sefton, E. M., Bhullar, B.-A. S., Mohaddes, Z. & Hanken, J. Evolution of the head–trunk interface in tetrapod vertebrates. *eLife* **5**, e09972 (2016).
30. Diogo, R. et al. A new heart for a new head in vertebrate cardiopharyngeal evolution. *Nature* **520**, 466–473 (2015).
31. Lescroart, F. et al. Clonal analysis reveals a common origin between nonsomite-derived neck muscles and heart myocardium. *Proc. Natl Acad. Sci. USA* **112**, 1446–1451 (2015).
32. Heude, E. et al. Unique morphogenetic signatures define mammalian neck muscles and associated connective tissues. *eLife* **7**, e40179 (2018).
33. Stensiö, E. A. *The Downtonian and Devonian Vertebrates of Spitsbergen, I: Family Cephalaspidae* (Dybwad, 1927).
34. Wängsjö, G. *The Downtonian and Devonian vertebrates of Spitsbergen. IX* (Norsk Polarinstitutt, 1952).
35. Shirai, S. Identity of extra branchial arches in Hexanchiformes (Pisces, Elasmobranchii). *Bull. Fac. Fish Hokkaido Univ.* **43**, 24–32 (1992).
36. Zhu, Y. et al. The oldest complete jawed vertebrates from the early Silurian of China. *Nature* **609**, 954–958 (2022).
37. Johanson, Z. & Smith, M. M. Placoderm fishes, pharyngeal denticles, and the vertebrate dentition. *J. Morphol.* **257**, 289–307 (2003).
38. Zangerl, R. *Handbook of Paleoichthyology, Vol. 3A Chondrichthyes I* (Gustav Fisher Verlag, 1981).
39. Coates, M. I., Gess, R. W., Finarelli, J. A., Criswell, K. E. & Tietjen, K. A symmoriiform chondrichthyan braincase and the origin of chimaeroid fishes. *Nature* **541**, 208–211 (2017).
40. Frey, L., Coates, M. I., Tietjen, K., Rücklin, M. & Klug, C. A symmoriiform from the Late Devonian of Morocco demonstrates a derived jaw function in ancient chondrichthyans. *Commun. Biol.* **3**, 681 (2020).
41. Anderson, P. S. L. & Westneat, M. W. Feeding mechanics and bite force modelling of the skull of *Dunkleosteus terrelli*, an ancient apex predator. *Biol. Lett.* **3**, 77–80 (2007).
42. Dearden, R. P., Stockey, C. & Brazeau, M. D. The pharynx of the stem-chondrichthyan *Ptomacanthus* and the early evolution of the gnathostome gill skeleton. *Nat. Commun.* **10**, 2050 (2019).
43. King, B., Qiao, T., Lee, M. S. Y., Zhu, M. & Long, J. A. Bayesian morphological clock methods resurrect placoderm monophyly and reveal rapid early evolution in jawed vertebrates. *Syst. Biol.* **66**, 499–516 (2017).
44. Rücklin, M. et al. Acanthodian dental development and the origin of gnathostome dentitions. *Nat. Ecol. Evol.* **5**, 919–926 (2021).
45. Naumann, B., Warth, P., Olsson, L. & Konstantinidis, P. The development of the cucullaris muscle and the branchial musculature in the Longnose Gar, (*Lepisosteus osseus*, Lepisosteiformes, Actinopterygii) and its implications for the evolution and development of the head/trunk interface in vertebrates. *Evol. Dev.* **19**, 263–276 (2017).
46. Kuratani, S. A muscular perspective on vertebrate evolution. *Science* **341**, 139–140 (2013).
47. Janvier, P. *Norselaspis glacialis* n.g., n.sp. et les relations phylogénétiques entre les kiaeraspidiens (Osteostraci) du Dévonien inférieur du Spitsberg. *Palaeovertebrata* **11**, 19–131 (1981).
48. Dupret, V., Sanchez, S., Goujet, D. & Ahlberg, P. E. The internal cranial anatomy of *Romundina stellina* Ørvig, 1975 (Vertebrata, Placodermi, Acanthothoraci) and the origin of jawed vertebrates—Anatomical atlas of a primitive gnathostome. *PLoS ONE* **12**, e0171241 (2017).
49. Goujet, D. & Young, G. C. in *Recent Advances in the Origin and Early Radiation of Vertebrates* (eds Arratia, G., Wilson, M. V. H. & Cloutier, R.) 109–126 (Verlag Dr Friedrich Pfeil, 2004).
50. Jarvik, E. *Basic Structure and Evolution of Vertebrates*, Vol. 1 (Academic Press, 1980).

Methods

Additional specimen

We analysed an articulated specimen of *Romundina* from the Geowissenschaftliches Zentrum der Universität Göttingen, Museum & Collection (GZG) specimen 100–488A.

Computed tomography scanning

We used x-ray computed microtomography to scan specimens of *Kolymaspis* and *Romundina*. We scanned the *Kolymaspis* specimen TsNIGR 7656 at the Natural History Museum (Imaging and Analysis Centre), UK using the Nikon Metrology HMX ST 225 system, 210 kV, 150 mA, 2.5 mm copper filter, and resulting voxel size of 70 µm. The *Romundina* specimen was scanned at the Cambridge University Museum of Zoology, using the Nikon Metrology HMX ST 225 system, 185 kV, 245 mA, 0.75 mm copper filter, and resulting voxel size of 43 µm.

Osteostracan tomography

To explore osteostracan vascularization patterns, we created a tomographic image series from the digitized publication of Stensiö (1927)[33]. We used Series F of *Mimetaspis hoeli* in plates 106–112, cropping each slice using Adobe Photoshop and exporting each to a separate bitmap file. We then loaded the series into SPIERS Align[51] and conducted a manual registration.

Segmentation and surface model visualzation

We performed segmentation of the tomographic datasets using Materialise Mimics (https://www.materialise.com). We segmented *Kolymaspis* primarily using Mimics v. 18; we finalized and cleaned the masks using Mimics v. 24. We segmented *Mimetaspis* series F, *Romundina* specimen GZG 100–488A, and existing data of *Brindabellaspis* (Extended Data Fig. 1) using Mimics v. 25. We used cycles rendering in Blender (Blender Foundation, https://www.blender.org) to generate surface model images for publication-ready figures.

Phylogenetic data

We used the dataset of King et al. [43] as the basis of our phylogenetic analysis, edited in Mesquite v 3.70[52]. It contains fully annotated character names and state labels. The removal of citation histories complicates dataset comparison and incorporation of new characters and data. Subsequent datasets have extinguished the records for many characters, resulting in incomplete character ontologies. This makes it nearly impossible for subsequent investigators to expand based on existing characters or to understand the original authors' intentions. We generated a change log using a newly developed command line tool diffmatrix (https://github.com/mbrazeau/diffmatrix/releases/tag/v2.2).

To preserve character histories and ontologies, we did not permanently delete any taxa or characters from the matrix. Rather than deleting characters or taxa we considered problematic, we preserved the overall integrity of the matrix by using exclusion settings before phylogenetic analysis. Instead of attaching the phylogenetic data file as separate character list and matrix, we have stored it as a single Nexus file in a version-control archive (GitHub) as a way of improving maintainability (https://mbrazeau.github.io/gnathostome_characters). This also includes a link to a character list web page with character descriptions and citations. Changes to the matrix are detailed in the change log at https://mbrazeau.github.io/gnathostome_characters/changelog.html. A permanent version of the final dataset used in this study is archived at https://github.com/mbrazeau/gnathostome_characters/releases/tag/1.0 and a copy of the Nexus file is provided in the Supplementary Information.

Phylogenetic analysis

We conducted a phylogenetic search using TNT (v. 1.6)[53]. We constrained the outgroup so that osteostracans and jawed vertebrates were each monophyletic. Because TNT constraints cannot conflict with outgroup choice, we later rerooted the trees so that Galeaspida were also monophyletic. Because all character types are symmetric this has no impact on the results. We set the tree buffer to 10,000 trees (hold 10000;) for unconstrained searches and up to 50,000 for searches under different constraints for placoderm monophyly. We conducted a 'new technology search' with the following command and settings to apply 50 iterations on the parsimony ratchet: xmult=level 10 ratchet 50; To further explore the resulting islands, we used additional branch-breaking (bbreak=fillonly;) to swap the trees in memory. We then computed the strict consensus tree using the nelsen command. We conducted two additional searches constraining placoderms to be monophyletic. The first constrained as monophyletic all placoderms inclusive of *Entelognathus* and *Minjinia*, while the second constrained only the 'core' placoderms[54] (excluding *Entelognathus* and *Minjinia* from the placoderm constraint).

Reporting summary

Further information on research design is available in the Nature Portfolio Reporting Summary linked to this article.

Data availability

Scan data and relevant surface meshes of *Kolymaspis* and *Romundina* are provided on FigShare (https://doi.org/10.6084/m9.figshare.22579840). The character list is stored in the original Nexus file, including character descriptions and references. Readers can access the file at https://mbrazeau.github.io/gnathostome_characters/ or in the Supplementary Information. Changes to the matrix are detailed in the change log at https://mbrazeau.github.io/gnathostome_characters/changelog.html.

Code availability

All TNT commands and scripts used in our analyses are provided in the Supplementary Information. Diffmatrix v2.2 used to generate the matrix change log is available as both source code and both macOS and Windows executables from https://github.com/mbrazeau/diffmatrix/releases/tag/v2.2.

51. Sutton, M. D., Garwood, R. J., Siveter, D. J. & Siveter, D. J. SPIERS and VAXML: a software toolkit for tomographic visualisation and a format for virtual specimen interchange. *Palaeontol. Electron.* **15**, 5T,14p (2012).
52. Maddison, D. R. & Maddison, W. P. Mesquite: a modular system for evolutionary analysis. Version 3.81 http://www.mesquiteproject.org (2021).
53. Goloboff, P. A. & Morales, M. E. TNT version 1.6, with a graphical interface for MacOS and Linux, including new routines in parallel. *Cladistics* **39**, 144–153 (2023).
54. King, B. & Rücklin, M. A Bayesian approach to dynamic homology of morphological characters and the ancestral phenotype of jawed vertebrates. *eLife* **9**, e62374 (2020).

Acknowledgements The authors thank A. Gehler for access to collections and R. Garwood and M. Sutton for technical support with SPIERS. TNT is made freely available with the support of the Willi Hennig Society. Computed tomography scanning of *Kolymaspis* was performed with the help of F. Ahmed at the Imaging and Analysis Centre, Natural History Museum, UK; computed tomography scanning of *Romundina* was performed by K. Smithson at the Cambridge Biotomography Centre, Department of Zoology, University of Cambridge. Original tomography and segmentation were supported by European Research Council Starting Grant under the European Union's Seventh Framework Programme (FP/2007–2013)/ERC Grant Agreement no. 311092 (M.D.B.) and the John Fell Fund, University of Oxford (M.F.). A.O.I. was supported by the Kazan Federal University Strategic Academic Leadership Program (PRIORITY-2030).

Author contributions Conceptualization: M.D.B. Methodology: M.D.B., M.C., M.F., A.E.F.E.F. and L.H. Investigation: M.D.B., M.C., A.E.F.E.F. and L.H. Visualization: M.D.B., M.C., A.E.F.E.F., L.H. and M.F. Funding acquisition: M.D.B. and M.F. Specimen access and geological data: A.O.I. Project administration: M.D.B. Supervision: M.D.B. Writing of original draft: M.D.B. Writing (review and editing): M.D.B., M.F. and Z.J.

Competing interests The authors declare no competing interests.

Additional information

Supplementary information The online version contains supplementary material available at https://doi.org/10.1038/s41586-023-06702-4.

Correspondence and requests for materials should be addressed to Martin D. Brazeau.

Peer review information *Nature* thanks Min Zhu and the other, anonymous, reviewer(s) for their contribution to the peer review of this work.

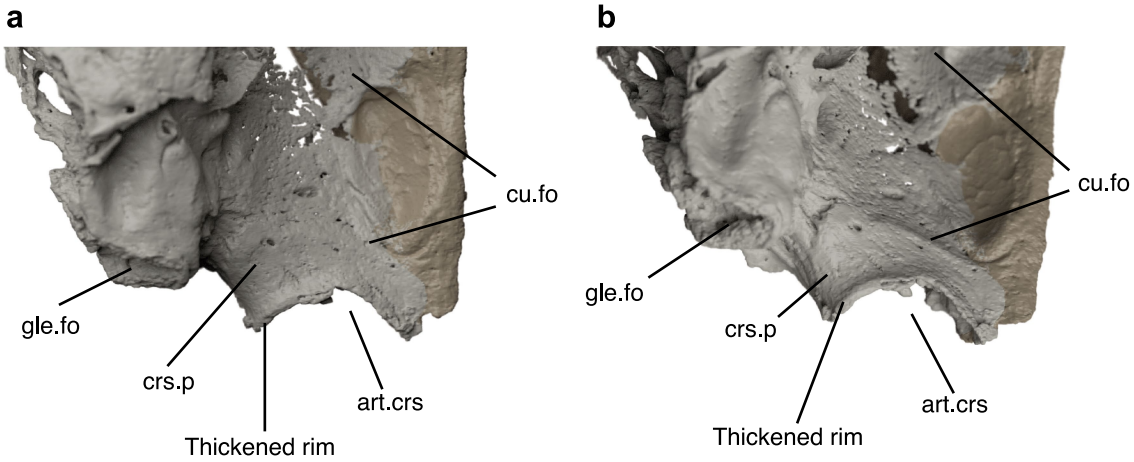

Extended Data Fig. 1 | Craniospinal process area of *Brindabellaspis* (Australian National University specimen 49493) showing the structure of the articular facet. a, Ventral view. **b**, Oblique posteroventral view. Abbreviations as in Fig. 1. Original segmentation of data from (ref. 26). Colour convention as in Fig. 1 (Main Text).

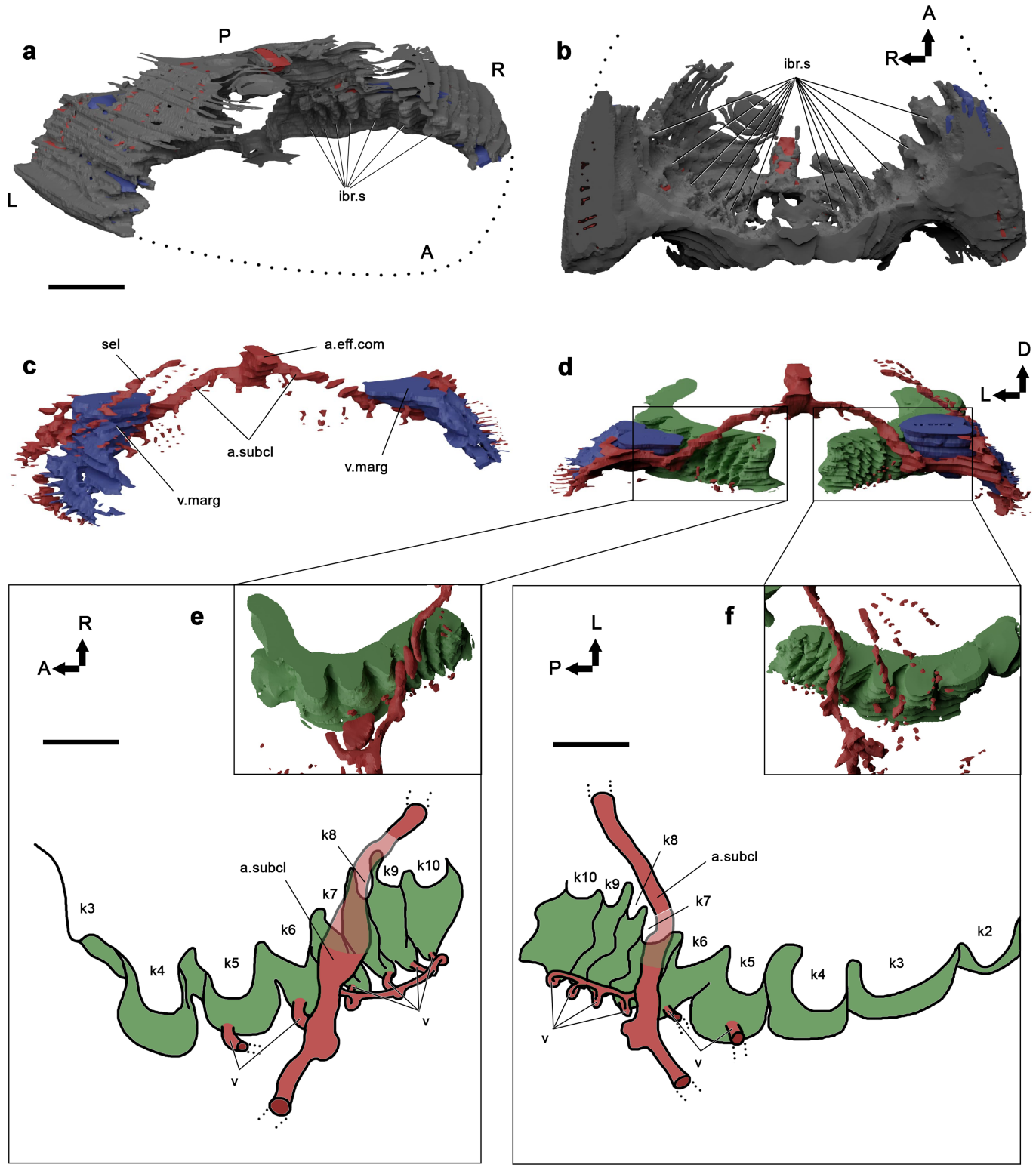

Extended Data Fig. 2 | Posterior section of the skull and endocast of the osteostracan *Mimetaspis hoeli* showing the position of the subclavian artery relative to the gill compartments. a, Skull. **b**, Ventral view of the skull. **c**, Endocast of blood vessels and 'sel' canals. **d**, Posterior view of the endocast and branchial space. **e**, Dorsal view of the left side arteries and branchial space. **f**, Dorsal view of the right side arteries and branchial space. **a** and **c** are from the same view. Additional abbreviations: a.eff.com, common efferent artery (dorsal aorta); ibr.s, interbranchial septa; k2–k10, pharyngeal cavities; sel, sensory field canals; v, canals for vessels; v.marg, marginal vein cavities. Colour scheme: dark grey, bone; red, small canals; blue, large canals and cavities; green, branchial space. Dotted lines indicate where the continuation of the specimen would be if it was complete. The arrows indicate the orientation of the specimen: A, anterior; D, dorsal; L, left; P, posterior; R, right. Top left scale bar is for **a**, **b** and **c** and equals 6 mm. Bottom left scale bar is for **e** and equals 3 mm. Bottom right scale bar is for **f** and equals approximately 4 mm.

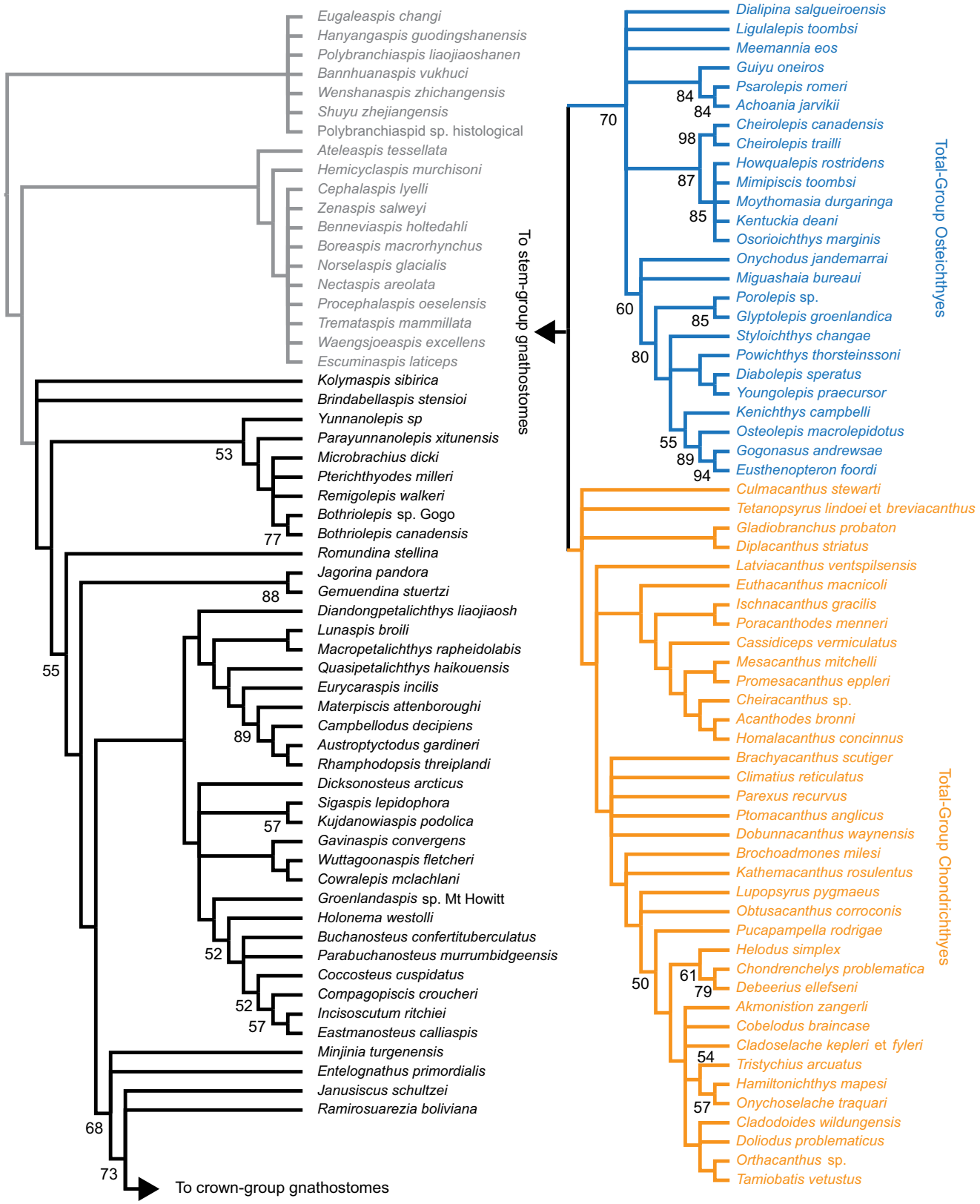

Extended Data Fig. 3 | Strict consensus tree from equal weights parsimony analysis. Outgroup (jawless vertebrates) shown in light grey. See supplementary information for details of tree number and tree score. Numbers below nodes show bootstrap values 50% or above.

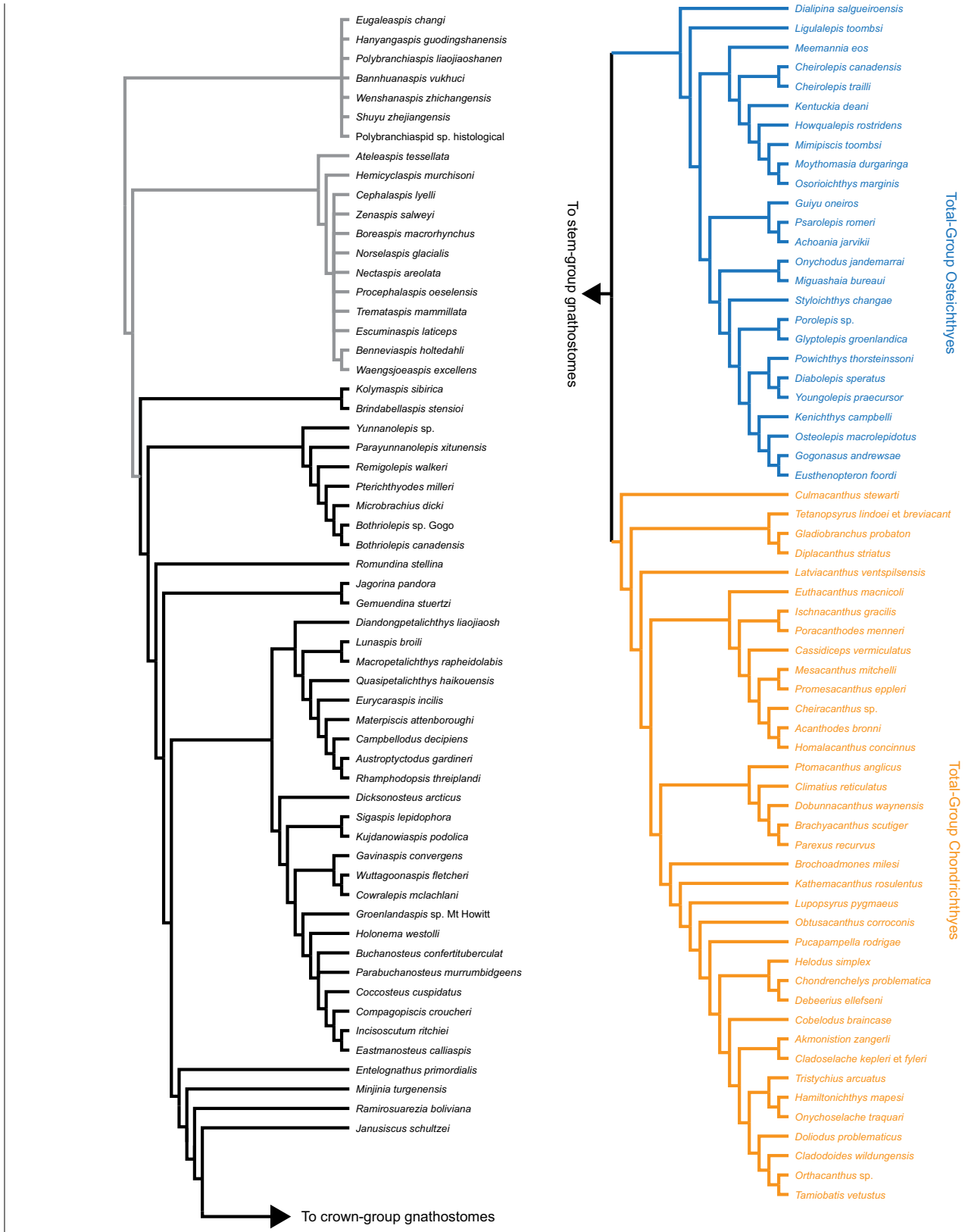

Extended Data Fig. 4 | Strict consensus tree from implied weights (k = 12) parsimony analysis. Outgroup (jawless vertebrates) shown in light grey. See supplementary information for details of tree number and tree score.

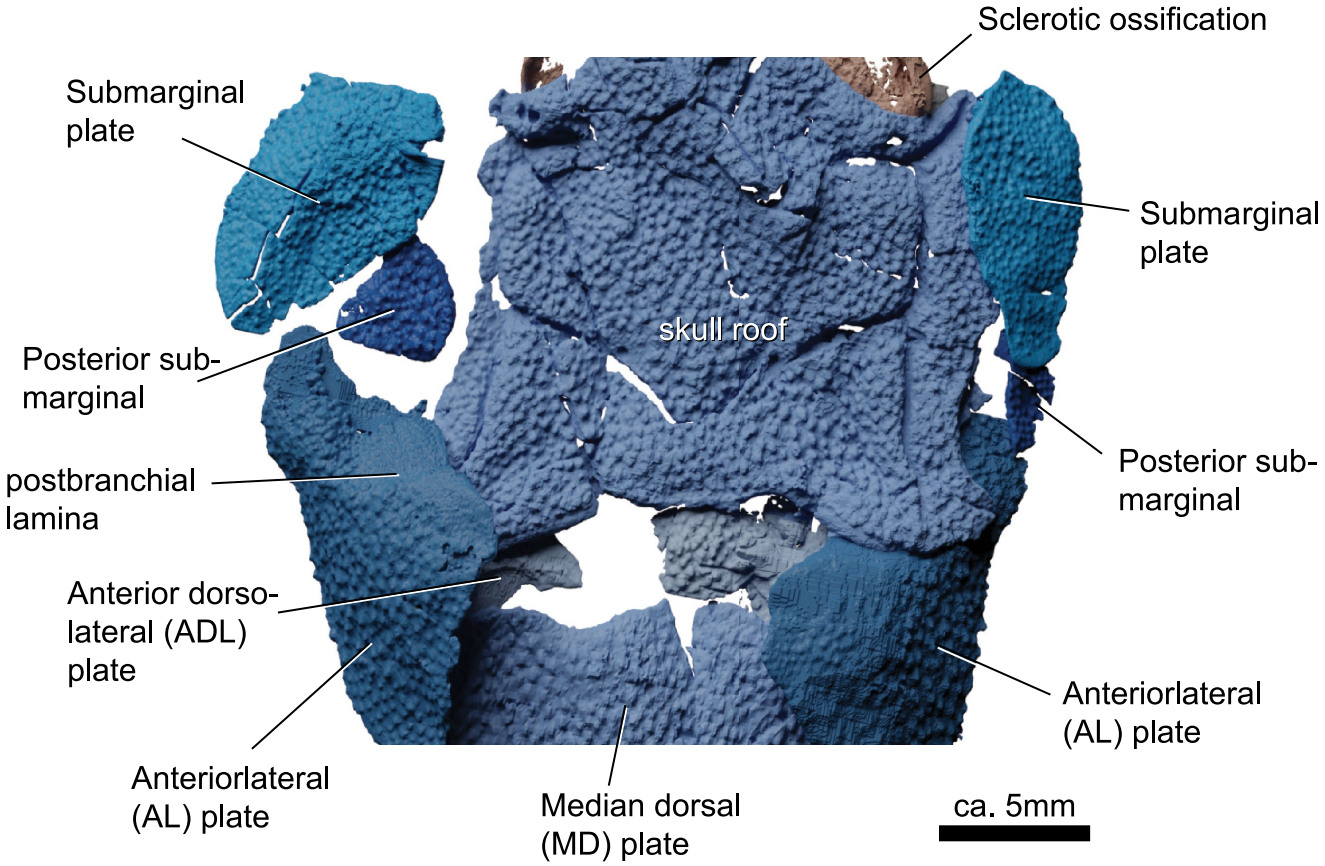

Extended Data Fig. 5 | *Romundina* sp. specimen GZG 100–488A showing multiple bony elements in opercular series.

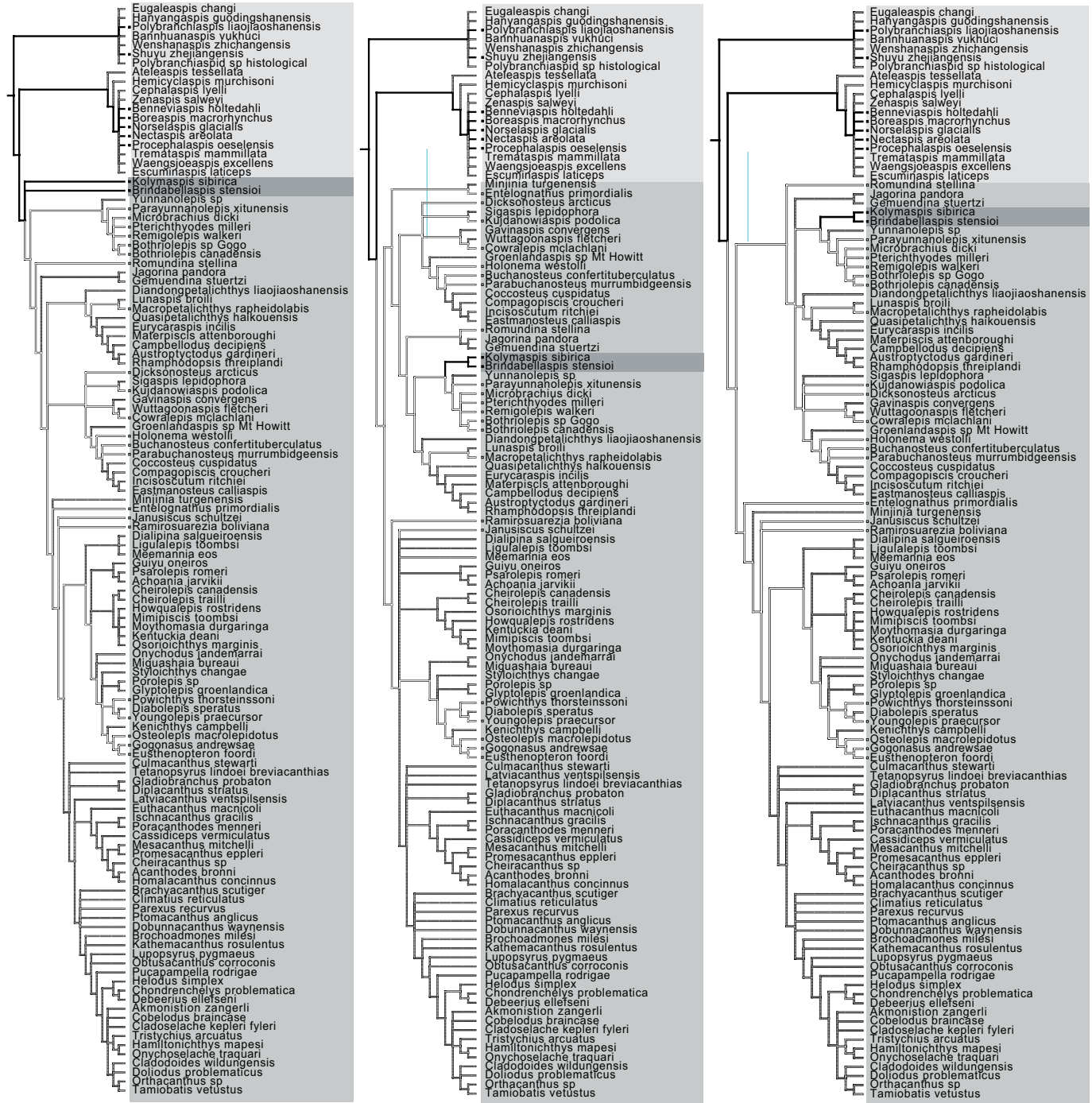

Extended Data Fig. 6 | Gnathostome phylogeny under two constraints on placoderm monophyly. Left, strict consensus tree of equally weighted parsimony analysis.Centre, all placoderms inclusive of *Entelognathus* and *Minjinia* constrained as a clade; Right, "core placoderms" (excluding *Entelognathus* and *Minjinia*) constrained as a clade. Colour coding shows parsimony ancestral states mapping for character 180 (Endoskeletal craniothoracic [sixth branchial] facet). Black: present; white: absent; gray: ambiguous.

nature portfolio

Corresponding author(s): Martin D Brazeau

Last updated by author(s): Sep 13, 2023

Reporting Summary

Nature Portfolio wishes to improve the reproducibility of the work that we publish. This form provides structure for consistency and transparency in reporting. For further information on Nature Portfolio policies, see our Editorial Policies and the Editorial Policy Checklist.

Statistics

For all statistical analyses, confirm that the following items are present in the figure legend, table legend, main text, or Methods section.

n/a	Confirmed	
☐	☒	The exact sample size (*n*) for each experimental group/condition, given as a discrete number and unit of measurement
☒	☐	A statement on whether measurements were taken from distinct samples or whether the same sample was measured repeatedly
☒	☐	The statistical test(s) used AND whether they are one- or two-sided *Only common tests should be described solely by name; describe more complex techniques in the Methods section.*
☒	☐	A description of all covariates tested
☐	☒	A description of any assumptions or corrections, such as tests of normality and adjustment for multiple comparisons
☒	☐	A full description of the statistical parameters including central tendency (e.g. means) or other basic estimates (e.g. regression coefficient) AND variation (e.g. standard deviation) or associated estimates of uncertainty (e.g. confidence intervals)
☒	☐	For null hypothesis testing, the test statistic (e.g. *F*, *t*, *r*) with confidence intervals, effect sizes, degrees of freedom and *P* value noted *Give P values as exact values whenever suitable.*
☒	☐	For Bayesian analysis, information on the choice of priors and Markov chain Monte Carlo settings
☒	☐	For hierarchical and complex designs, identification of the appropriate level for tests and full reporting of outcomes
☒	☐	Estimates of effect sizes (e.g. Cohen's *d*, Pearson's *r*), indicating how they were calculated

Our web collection on statistics for biologists contains articles on many of the points above.

Software and code

Policy information about availability of computer code

Data collection	We performed segmentation of the tomographic datasets using Materialise Mimics (https://www.materialise.com). We segmented Kolymaspis was primarily using Mimics v. 18; we finalized and cleaned the masks using Mimics v. 24. We segmented Mimetaspis Series F and Romundina specimen GZG 100-488A using Mimics v. 25. We used cycles rendering in Blender 3.2.2 (Blender Foundation, https://www.blender.org) to generate surface model images for publication-ready figures. We used SPIERS Align v. 3.1 (Sutton et al.) and conducted a manual registration.
Data analysis	We conducted a phylogenetic search using TNT (v. 1.5) (Goloboff & Catalano 2015). We wrote a custom software tool diffmatrix v2.2 to compare our dataset to an earlier iteration. This has been made available through a link to GitHub: https://github.com/mbrazeau/diffmatrix (release version: https://github.com/mbrazeau/diffmatrix/releases/tag/v2.2)

For manuscripts utilizing custom algorithms or software that are central to the research but not yet described in published literature, software must be made available to editors and reviewers. We strongly encourage code deposition in a community repository (e.g. GitHub). See the Nature Portfolio guidelines for submitting code & software for further information.

Data

Policy information about availability of data

All manuscripts must include a data availability statement. This statement should provide the following information, where applicable:

- Accession codes, unique identifiers, or web links for publicly available datasets
- A description of any restrictions on data availability
- For clinical datasets or third party data, please ensure that the statement adheres to our policy

Scan data and relevant surface meshes of Kolymaspis and Romundina are provided deposited on FigShare (10.6084/m9.figshare.22579840). The character list is stored in the original Nexus file including character descriptions and references. Readers can access the file at https://mbrazeau.github.io/gnathostome_characters/ which also includes a link to a character list web page. Changes to the matrix are detailed in the change log at https://mbrazeau.github.io/gnathostome_characters/changelog.html . A permanent version of the final dataset is archived at (https://github.com/mbrazeau/gnathostome_characters/releases/tag/1.0-review).

Research involving human participants, their data, or biological material

Policy information about studies with human participants or human data. See also policy information about sex, gender (identity/presentation), and sexual orientation and race, ethnicity and racism.

Reporting on sex and gender	n/a
Reporting on race, ethnicity, or other socially relevant groupings	n/a
Population characteristics	n/a
Recruitment	n/a
Ethics oversight	n/a

Note that full information on the approval of the study protocol must also be provided in the manuscript.

Field-specific reporting

Please select the one below that is the best fit for your research. If you are not sure, read the appropriate sections before making your selection.

☐ Life sciences ☐ Behavioural & social sciences ☒ Ecological, evolutionary & environmental sciences

For a reference copy of the document with all sections, see nature.com/documents/nr-reporting-summary-flat.pdf

Ecological, evolutionary & environmental sciences study design

All studies must disclose on these points even when the disclosure is negative.

Study description	Anatomical descriptions of existing fossil material using computed tomography. This was supplemented with literature-based and collections-based comparative analysis.
Research sample	The main focus of this work was the braincase of the enigmatic placoderm fish, Kolymaspis sibirica from the Early Devonian of Siberia. This placoderm fish reveals a unique morphology of the head-shoulder linkage which provides clues to the relationship between the pharynx and shoulder in early gnathostomes.
Sampling strategy	n/a
Data collection	n/a
Timing and spatial scale	n/a
Data exclusions	n/a
Reproducibility	All specimens involved in this study are housed in permanent repositories. We have furthermore provided a complete digital archive of all relevant data required to reproduce the study.
Randomization	n/a
Blinding	n/a

Did the study involve field work? ☐ Yes ☒ No

Reporting for specific materials, systems and methods

We require information from authors about some types of materials, experimental systems and methods used in many studies. Here, indicate whether each material, system or method listed is relevant to your study. If you are not sure if a list item applies to your research, read the appropriate section before selecting a response.

Materials & experimental systems

n/a	Involved in the study
☒	☐ Antibodies
☒	☐ Eukaryotic cell lines
☐	☒ Palaeontology and archaeology
☒	☐ Animals and other organisms
☒	☐ Clinical data
☒	☐ Dual use research of concern
☒	☐ Plants

Methods

n/a	Involved in the study
☒	☐ ChIP-seq
☒	☐ Flow cytometry
☒	☐ MRI-based neuroimaging

Palaeontology and Archaeology

Specimen provenance	Kolymaspis sibirica is from the Magadan Oblast of far eastern Siberia. It was collected in the mid-20th century. The specimen of Romundina is from the Drake Bay formation on Prince of Wales Island, in what is now Nunavut. It was collected in 1975 by Hans-Peter Schultze and Frank Langenstrassen when the region was still part of the Northwest Territories.
Specimen deposition	Kolymaspis is deposited in the FN Chernyshev Central Research Geological Museum in St. Petersburg, Russia. Romundina specimen is housed in Geowissenschaftliches Zentrum der Universität Göttingen, Museum & Collection (GZG)
Dating methods	n/a

☐ Tick this box to confirm that the raw and calibrated dates are available in the paper or in Supplementary Information.

Ethics oversight	No ethical approvals were required as all material is housed in existing accredited collections .

Note that full information on the approval of the study protocol must also be provided in the manuscript.